https://dx.doi.org/10.22161/ijaers.5.6.23 *ISSN: 2349-6495(P) | 2456-1908(O)*

Design and Development of a Magnus Hydrokinetic Rotor

Rodrigo Paludo[1]*, Rodrigo C. Quadros[1], Gelson L. Carneiro[1], Paulo C. Moro[1], Tiago Francesconi[1], Paulo C. Pereira[2], Ricardo L. da Luz[2], Eduard N. Stutz[1], Carlo G. Filippin[1]

[1]Mechanical Department, Institutos Lactec, Curitiba, Brazil
[2]Eletrosul, Florianópolis, Brazil
*rodrigo.paludo@lactec.org.br

Abstract**—** *The energy matrix diversification has become noticed in the latest years. Energy conversion of the free flow in rivers and canals into electrical energy has been a good complementation for the conventional generation. The first application of hydrokinetic turbines, commercially, were in Mississippi's river (Minnesota, USA), in 2008. The usage of Magnus effect in hydrokinetic turbines occurred in an innovative manner. In this project, rotational cylinders actuate as blades of an axial hydrokinetic rotor, converting kinetic energy of the flow into potency in the rotor axle. This effect was initially observed in 1853 by Henrich Magnus and, since then, few researches were carried out to its application in hydraulic generation of energy. Therefore, tests in reduced-scale prototype and numerical simulations were made for the development and executive design of a hydrokinetic rotor. At the end of this study, a hydro generator with 62% hydraulic efficiency, considering the Betz Limit, was constructed.*

Keywords— Magnus Effect; Energy Generation; Numerical Simulation.

I. INTRODUCTION

Magnus effect was discovered in 1853 by the German physicist Heinrich Gustav Magnus, from University of Berlin (Reid, 1997). This phenomenon can be observed when axisymmetric bodies start rotating in a flowage. Thus, following the no-slip condition, one layer of the fluid is displaced in the same rotational direction of the body. This movement in the rotational direction is transferred to the slightly posteriors layers, what changes the pressure distribution next to the body, generating lift.

In 1920 the first notable application of the Magnus effect was carried out, by Anton Flettner, for Buckau's propulsion, a ship whose masts were rotational cylinders of 13 meters height and 2.7 meters diameter, with a rotational speed of up to 125 rpm. The masts were spun by electric motors, generating a resultant propulsion force that made Buckau capable to cross Atlantic Ocean in 1926 (Prandtl, 1925; Vieira, 1961).

In 2010 Magnus effect was employed in E-Ship1. This ship is used for the transportation of aero generators blades, and the effect had provided a reduction in fuel consumption of 30 to 40% (Wobben, 2010). An advantage of Magnus effect is that, depending on the work conditions, much larger lift forces are attainable when compared to those developed by conventional profiles with the same dimensions (Vieira, 1961).

The application of Magnus effect in hydraulic turbines hasn't been much studied yet, or, at least, not much disclosed. There's few literature about this theme – there is more literature about its application in aerogenerators (US 20070046029 A1, 2007), maritime propellers (Bergeson & Kent Greenwald, 1985), tennis (Goodwill, Chin, & Haake, 2004), golf and baseball (Nagami, Higuchi, Nakata, Yanai, & Kanosue, 2016) ball's deflection and its behavior on flowpast a rotating cylinder (Badr, Coutanceau, Dennis, & Mnard, 1990; Karabelas, 2010). Therefore, in this study established through the companies ELETROSUL and Institutos LACTEC, it was developed a contextualized approach about how this phenomenon manifests in water, identifying a potential application in the commercial electrical energy generation perspective.

Since its origin, hydrodynamic was very connected to direct investigation, experimentation, standing out the usage of aerodynamics tunnels as methods of trialling different wing's profiles. The main goals in theoretical and experimental studies were always to obtain the highest lift-drag ratio (Huang, Cheng, Chen, & Hsu, 2011; Tokumaru & Dimotakis, 1991; Vieira, 1961; Yen, San, & Chuang, 2008; Zhang, Wang, Lu, & Mi, 2005). For instance, Karabela (Karabelas, Koumroglou, Argyropoulos, & Markatos, 2012) studied the influence of the cylinder rotating speed on lift and drag coefficients, finding that the best aspect ratio, defined as the ratio between the circumferential velocity of the cylinder and the free-stream velocity, is 2.

Different diameters cylinders were employed in this study, which allowed the designation of the best aspect ratio, ratio of length to radius, in view of a future application. The

https://dx.doi.org/10.22161/ijaers.5.6.23 *ISSN: 2349-6495(P) | 2456-1908(O)*

experimental results are compared to the theoretical obtained through the use of the equations based on the Kutta-Joukowsky theorem.

Subsequently to the theoretical and the cylinders' studies, separately, tests were performed in a reduced-scale model, as well as in numeric simulations to establish the best geometric arrangement of the device.

II. MATERIALS AND METHODS

Usually, the main goals of the aerodynamic profile's studies are the enlargement of the lift coefficient and the reduction of the drag coefficient. The choice of one model of profile, between various existent types, is normally done using a curve that relates lift coefficient (CL) with the drag coefficient (CD) and varying the angle of attack (Mannini, Marra, Pigolotti, & Bartoli, 2017; Robertson, Wedding, Peterka, & Cermak, 1977), which can be defined as the inclination of the profile in relation to the flow direction. Naturally, a cylindrical profile doesn't have an angle of attack that can be modified, as in a wing profile, being the lift of the cylindrical profile usually obtained as a consequence of a rotation that is inferred to the cylinder and changes his circulation.

Therefore, based on the Kutta-Joukowski theorem, the lift per unit of length (L) of a cylinder can be determined by the equation (1) (Lugones, 2011):

$$L = \rho_{\infty}.V_{\infty}.\Gamma \quad (1)$$

Where,

L → lift force per unit of length [N/m];

ρ_{∞} → specific weight of the fluid of the free flow [kg/m^3];

V_{∞} → speed of the free flow[m/s];

Γ → circulation [m^2/s].

Fig. 1: Photo sequence of flowage's visualization by dye injection

The circulation is a scalar quantity associated to the vorticity. Fig. 1 presents an image sequence of the experiment discussed in this work, wherein can be verified, through the dye injection method, the circulation of the fluid around the rotational cylinder.

Mathematically, the circulation is given by (2) (Anderson, 1991):

$$\Gamma = \oint \vec{V} \cdot d\vec{s} \quad (2)$$

With,

$\vec{V}$ → speed along a streamline [m/s];

$d\vec{s}$ → infinitesimal length of a streamline [m].

Thus, in (1), integrating from 0 to 2π, the equation (3) of the circulation around the cylinder (Munson, Young, & Okiishi, 2004) is obtained:

$$\Gamma = 2.\pi.\omega.r^2 \quad (3)$$

With,

ω → angular speed [rad/s];

r → cylinder radius [m].

Hence, replacing equation (3) in (2), the lift force of the cylinder per unit of length can be obtained.

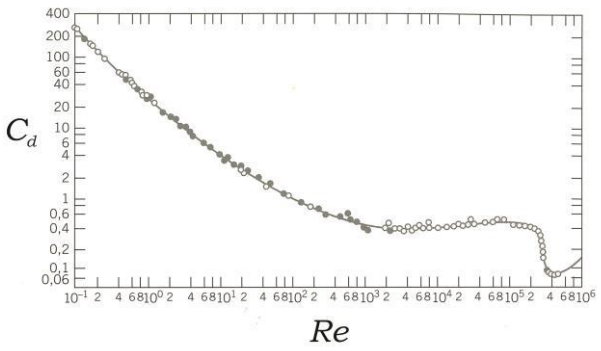

Fig. 2: Drag coefficient, as a function of Reynolds number, for a smooth cylinder (Anderson, 1991)

The drag on a body that moves through a certain liquid can be comprehended as a quantity of restriction force to its free movement, which increases along with the relative speed between the body and the fluid.

The D'Alembert Paradox (D'Alembert, 1768) establishes that the drag on a cylinder placed in the interior of an ideal fluid (not viscous) is null, due to the balance of forces established as a result of the flow uniformity along the symmetry that exists between the two parts of the cylinder. However, the results obtained experimentally oppose the Paradox, once any real fluid have viscosity which will originate, due to the existent shear forces between the fluid particles, drag forces on the cylinder.

https://dx.doi.org/10.22161/ijaers.5.6.23 *ISSN: 2349-6495(P) | 2456-1908(O)*

In such manner, the drag force on a cylinder is obtained, classically, by means of the equation (4), using an experimental coefficient educed from the curve presented in Fig. 2.

$$F_a = \frac{1}{2}.\rho.A.V^2.C_d \quad (4)$$

With,
F_a → drag force [N]
ρ → fluid specific weight [kg/m³];
A → area [m²];
V → relative speed between the fluid and the body [m/s];
C_d → drag coefficient;
Re → Reynolds number;
μ → dynamic viscosity [Pa.s];
D → cylinder diameter [m].

The drag coefficient (C_d) is obtained from an experimental curve that sets up a correlation between the coefficient values and the Reynolds number.

III. EXPERIMENTAL DEVELOPMENT

The experimental development was based on the construction of an arrangement for the measurement of the perpendicular forces, drag and Magnus (lift), which actuate on the rotational cylinder. The experiment was performed in a canal whose flow rate was able to be controlled. The forces measurement arrangement, utilized on the trial, was fixed on the systems base, as in Fig. 3.

Therefore it became possible to measure the active forces on each one of the six cylinders employed, whose characteristics are shown in Table 1.

The nomenclature was defined as (C) for cylinder and subsequently the number, which represents the increasing order of the diameter. The (R) presented in C3R represents the knurled surface of the cylinder, whose goal was to evaluate the influence of the roughness on the Magnus effect as well as on the drag.

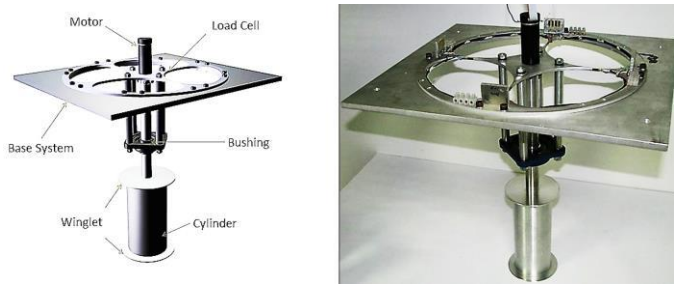

a *b*

Fig. 3: Measurement arrangement.
(a) Schematic image, (b) Photograph of the constructed load cell.

Table 1: Data table of the studied cylinders

Nomenclature	Length (mm)	Diameter (mm)	Aspect ratio
C1	200	33.20	12.05
C2		48.95	8.17
C3		63.55	6.29
C3R		63.55	6.29
C4		76.90	5.20
C5		100.70	3.97

Thus, two cylinders with same diameter were built, one with a smooth surface and the other with a knurled surface.

$$a = l/r \quad (5)$$

Where:
a → aspect ratio (dimensionless);
l → cylinder length;

The tests were carried out varying the following parameters:
1) cylinders' angular speed;
2) diameter;
3) water flow velocity;
4) roughness.

According to the equation (6), as smaller the cylinder radius is, greater should be the angular speed in order that, in a flow of constant speed, the specific rotation is remained constant.

$$\alpha = \frac{\omega.r}{V_\infty} \quad (6)$$

Where,
α → specific rotation [dimensionless].

Thus, the experimental procedure was comprehended as the establishment of the canal's water level in 300 mm and, in condition of no flow, the definition of the force measurement system ground zero, eliminating other variables as thrust. After resetting the load cell with no water flow, the next step was to open the input valve and establish the adequate flow rate to reach a stipulated velocity, first of 0.2 m/s and then, similarly, of 0.4 m/s.

Previously to the test's beginning, with the cylinder in stationary condition, a sample of Magnus and drag forces' values was recorded. Afterwards, the measurement system was reset once more, though this time in presence of flow, in order to establish the ground zero on Magnus force and, also, a measured value of drag. This measured value of drag force, obtained in presence of flow and without rotation, was added up to each case obtained subsequently, with rotation. That was made because, before obtaining the measurement for each rotation, the system was reset,

https://dx.doi.org/10.22161/ijaers.5.6.23 *ISSN: 2349-6495(P) | 2456-1908(O)*

suppressing the portion of drag existent without rotation. Nevertheless, the values of residual Magnus force existent, obtained in presence of flow and without rotation, were discounted in each case, maintaining so the coherence of measurement's purpose.

After the experiment in the tests channel, several warheads geometries were simulated with the software Star CCM+. The aim was to define which model presents the lowest drag. With the constructive parameters determined, the hydro generator was designed and built.

IV. RESULTS AND DISCUSSIONS

Fig. 4*a* presents values of Magnus and drag forces for each cylinder, with a flow velocity of 0.2 m/s and distinct rotating speeds. It's important to notice that the curves presented in the figures are the tendency of a cloud of points collected from the measurement system. It could be observed that C1, besides inserting a great vibration to the system, can also provide low values of forces, for both Magnus and drag, what requested a refined treatment of this data, keeping, however, a random error inserted in its final results. Otherwise, the same wasn't found in the other cylinders. Therefore, it was verified that the usage of a cylinder with a larger diameter solved the vibration's problem.

Fig. 4*b* shows the Magnus and drag forces values, for each cylinder in flow velocity of 0.4 m/s and different rotation speeds. Analysing this figure, a difference in the forces applied on the cylinders is noticeable when compared to the forces plotted in Fig. 4*a*. It's clear that this alteration occurs due to the increase of the flow velocity, which means: Magnus and drag forces are functions of the flow speed.

It's noticed, in Fig. 4*a*, that Magnus force have a slight increase in C3R when compared to C3, but this behavior changes for 0.4 m/s flow, conform presents Fig. 4*b*.

On account of the greater coherence of data for larger flow velocity, from this point forward more emphasis will be given to the data collected with 0.4 m/s of velocity in the canal.

The specific rotation gives an idea of relative speed between the tangential velocity, in the cylinder external surface, and the velocity of free flow. This correlation suggests a pressure difference between the two counter faces of the cylinder, perpendiculars to the flow. Thus, that would be the origin of Magnus force, whose maximum value should be the same for two identical diameter cylinders in the same rotation or specific rotation. Particular comparison was made for cylinders C3 and C3R, of equal diameter, which differentiate just by the fact that the C3R have a knurled surface, which, in turn, propitiates a greater rugosity in comparison to C3. The curves plotted in Fig. 5 present the values of CL and CD, as a function of the specific rotation, for the two cylinders.

Fig. 5 shows that C3R have a maximum lift force value with a specific rotation of 6 (720 rpm), dissimilar to cylinder C3, in which the lift force appears around 5 (610 rpm). To obtain an equal lift value, the cylinder C3 needs a lower rotation and, there so, presents a smaller consumption in comparison to C3R, which clarifies that, in this experiment, rugosity diminished the system efficiency.

It should be highlighted that, as well as a wing have tendencies that repeat in scale, the cylinders have very near tendencies. That is, it also repeats in scale. Thus, all cylinders present similar behavior which varies, in most part of the time, only in module. This fact is evidenced by the data obtained from the different cylinders and, even more, by C3R's behavior, which is slightly different in consequence of its dissimilar rugosity. C3R would be the one cylinder, in the present study, that doesn't vary its behavior only in scale. This tendency is more evident when CL and CD are analyzed, which are presented in Fig. 6 as a function of the specific rotation, for a 0.4 m/s velocity.

One more time, it is evident the difference between the C3R and the others. Through the analysis of the graphics in Fig. 6 - except for C3R - the specific rotation expected for the maximum CL stayed very close to five, whereas for C3R it was around six.

Other carried out analysis was the evaluation of the resultant between Magnus and drag forces, supposing that both are actuating in the same direction with opposite orientation. In this case, it is observed that the Magnus and drag forces are perpendicular to each other and were subtracted, just as a form of assess which cylinder presents better relation between these two forces.

From the comprehensive indicators of Table 2 and Table 3, the operational rotation speed, for a greater resultant force per cylinder, doesn't coincide with the maximum Magnus force, remaining in all cases at a slightly lower rotation.

In Table 2 and Table 3, for a criterion analysis, adopting the cylinder four (C4) as example, it's verified that in maximum Magnus force, which occurs in this case at 540 rpm, the resultant between Magnus and drag had a modulus of around 0.34 kgf. However, the highest difference between Magnus and drag doesn't occur coincidently with the maximal rotation, presenting a 440 rpm value to achieve the maximum resultant force.

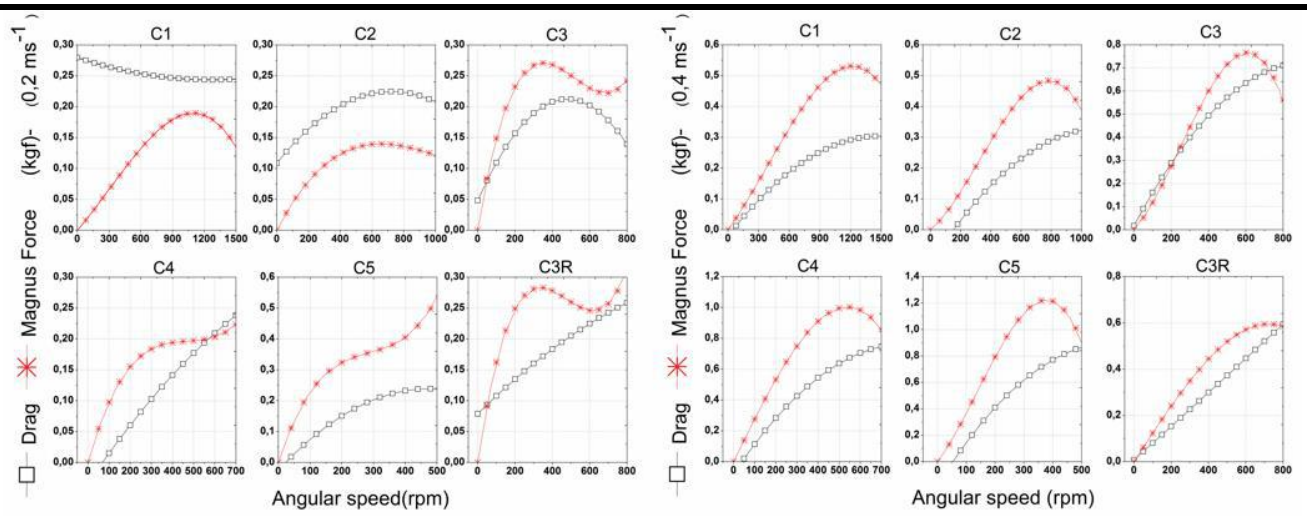

a *b*

Fig. 4: Graphics of drag and Magnus forces for different flow velocities. (a) Measured for 0.2 m/s, (b) Measured for 0.4 m/s.

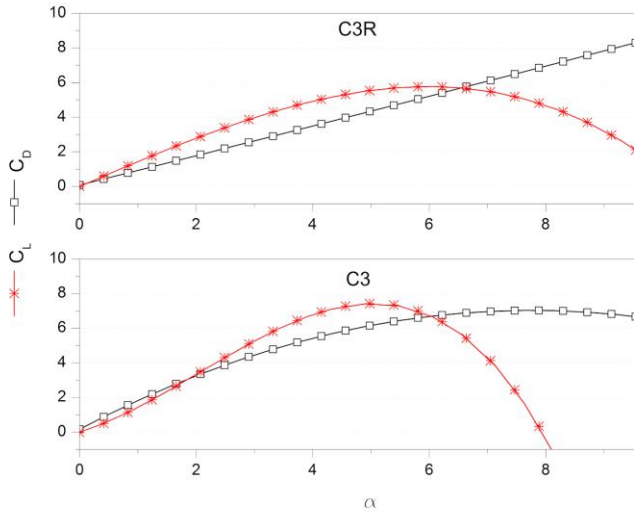

Fig. 5: Variation of CL and CD under different specific rotations, for C3 and C3R.

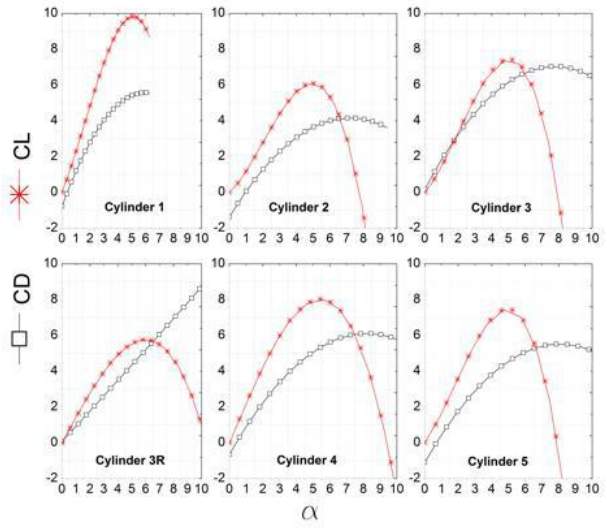

Fig. 6: Coefficients CL and CD in a flow velocity of 0.4 m/s.

Table 2: Difference between maximum lift and Drag forces

Nomenclature	Rotational speed (rpm)	Difference $F_{Lmax} - F_D$ (kgf)
C1	1220	0.24
C2	790	0.20
C3	610	0.13
C3R	720	0.06
C4	540	0.34
C5	380	0.48

Table 3: Maximum difference between lift and Drag forces

Nomenclature	Rotational speed (rpm)	Difference $F_L - F_D$ (kgf)
C1	1150	0.25
C2	700	0.21
C3	530	0.15
C3R	460	0.15
C4	440	0.37
C5	330	0.52

https://dx.doi.org/10.22161/ijaers.5.6.23 *ISSN: 2349-6495(P) | 2456-1908(O)*

Fig. 7 presents the consumption's variation of the electric motors, employed to rotate the cylinders, as a function of the specific rotation. In this study, consumption enlarged as the aspect ratio diminishes. The values obtained for C1, slenderer, clearly can't be considered, mainly due to imbalance and vibrations that occurred during the measurement. Particular attention should be given, one more time, to the C3R whose consumption overcame C4's, according to Fig. 7.

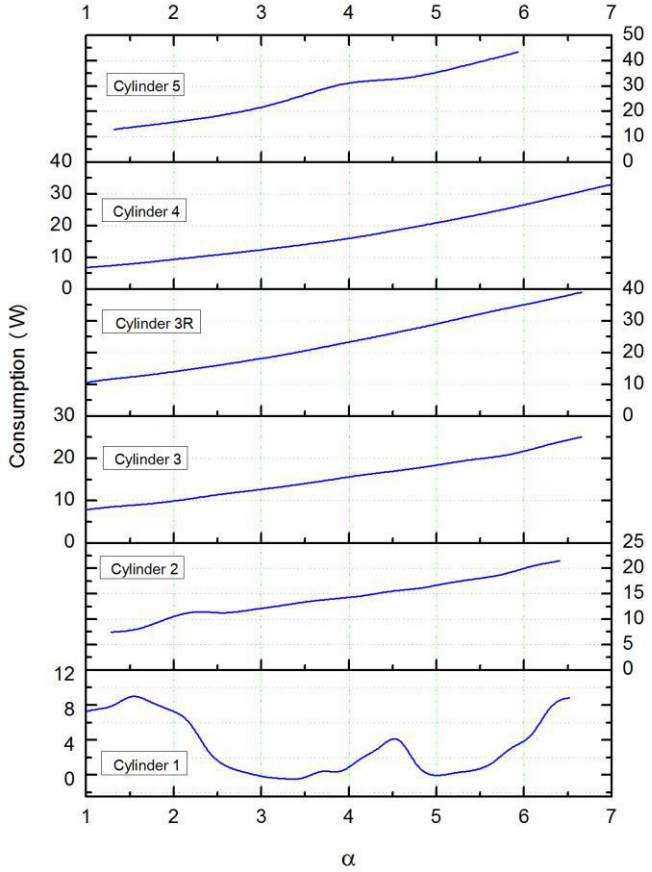

Fig. 7: Instantaneous consumption as a function of specific rotation, with a 0.4 m/s flow.

There so, for a more complete analysis that could, finally, point the most suitable aspect ratio in the current study, the following parameters were related in the same curve:

a) The maximal resultant force ($F_M - F_D$) that leads to the highest resultant torque pro cylinder;
b) The consumption in the rotation that maximizes the resultant force;
c) The rotation wherewith the maximum resultant forces are obtained;

Fig. 8 presents this curve, which reveals the relation between the three cited parameters.

Through the analysis of the curve in Fig. 8, it's plausible to admit that the greatest aspect ratio is obtained with C4. The C4, in relation to C5, operate almost in the same rotation, presenting a resultant force that is, in modulus, 32% lower. Moreover, C4 is more efficient than C5 because it consumes about 38% less. In sum, regarding the comparison with the others cylinders, the C4, in relation to:

C5 – Consumes 38% less and have a 32% smaller resultant;
C3R – Consumes less and the resultant is bigger;
C3 - Consumes slightly more and the resultant is bigger;
C2 - Consumes slightly more and the resultant is bigger.

Fig. 8 reveals a practically linear increase in consumption between the cylinders C2, C3 and C4. The same does not occur with the C5, what suggests that the increase stops being linear after a given cylinder diameter. Another relevant point is C3R's consumption, which tends to rise along with greater rugosity. Speed has an approximately quadratic diminishment with the cylinder diameter's growth, while the force's maximal difference initially decreases, reaching a minimum with the C3.

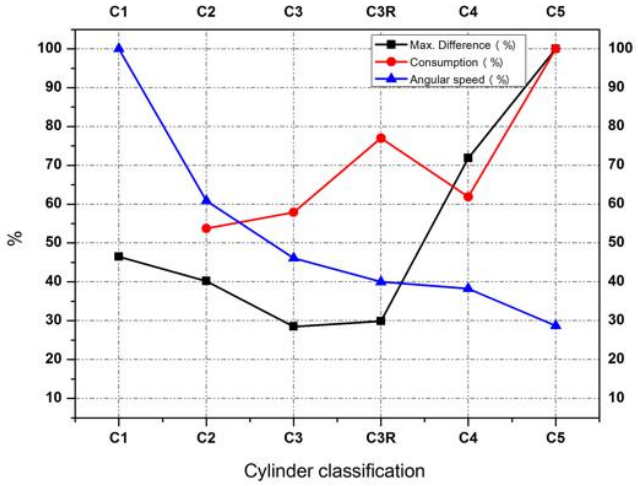

Fig. 8: Relation between consumption and Magnus-Drag efficiency.

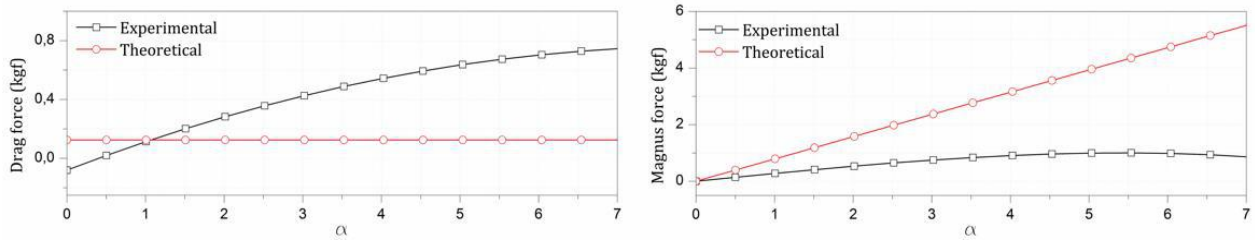

a *b*

Fig. 9: Differentiation between theoretical and experimental forces: (a) for drag force. (b) for Magnus force.

https://dx.doi.org/10.22161/ijaers.5.6.23 *ISSN: 2349-6495(P) | 2456-1908(O)*

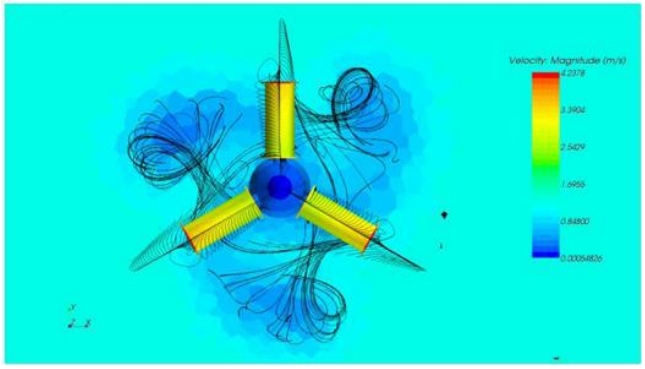

Fig. 10: Simulation of a complete rotor.

The theoretical results had shown significant differences in comparison with the experimentally achieved. According to Fig. 9*a*, there's a clear difference between the Magnus force, foreseen by theory, and the experimentally obtained for the C4's case, defined as the one with the suitable aspect ratio in the studies.

Fig. 11: Picture of the complete machine, set up over the canal.

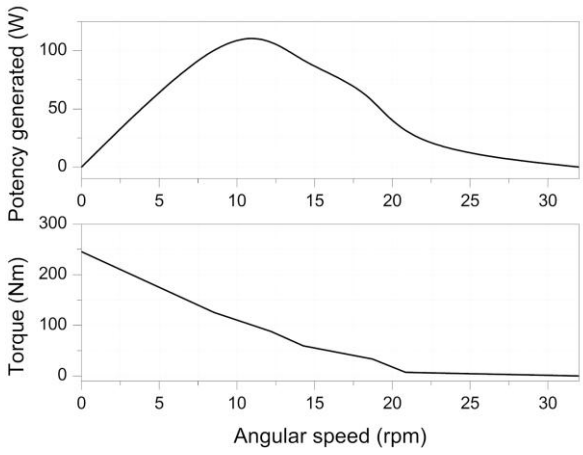

Fig. 12: Potency and torque of the machine.

Likewise, in Fig. 9*b* is verified the difference between theoretical and experimental drag force. This difference occurred, basically, because the classic theory of drag force, for a cylinder immersed in a fluid, doesn't consider the influence of its rotation.

At the start, the rotation of the cylinders was followed by a given vibration, which inserts an uncertainty to the measurement system. This, in turn, could justify the negative beginning of the drag force, as shown in Fig. 9*b*.

The cylinder that exhibited the greatest performance, the one with the aspect ratio 5.2 (C4), was constructed.

The simulations of the complete rotor, illustrated in Fig. 10, enabled the determination of the end-plate diameter and the ogive geometry.

There so, a hydro generator was built, based on the obtained parameters. To measure the torque of the machine, a Prony brake dynamometer was employed. Fig. 11 shows the machine set up over the canal.

In the same axle of the brake, an encoder was installed, in order to measure the machine's angular speed (ω). Fig. 12 presents the potency and torque obtained.

V. CONCLUSIONS

The performed trials intended to compare the aspect ratios of the cylinders. Based on these tests, the best aspect ratio could be selected according to the maximal Magnus resultant force criteria. Thus, between the tested aspect ratios, it's verified that the cylinder with the superior efficiency, by the adopted criteria, was the one with 5.2. It is important to emphasize that this aspect ratio will be used in the construction of a machine for electricity micro-generation, fact that motivated the trials performance.

The Magnus Effect has potential for applications in hydro kinetic machines. However, this technology hasn't attained its development apex yet. As an example there's the employment, not tested yet, of a diffuser which, according with recent studies, could increase the *Cp* (potency coefficient) in 43% (Brasil Júnior, 2007).

On the other hand, in the current conditions, there is a potential application for this technology, requiring, for its establishment, the specification of a suitable surrounding.

ACKNOWLEDGMENTS

The Institutos LACTEC extends thanks to the Institutions:
- ELETROSUL Centrais Elétricas S.A.
- Agência Nacional de Energia Elétrica - ANEEL.

REFERENCES

Anderson, J. D. (1991). *Fundamentals of Aerodynamics*. (L. Bearnesderfer & E. Castellano, Eds.) (2nd ed.). McGraw-Hill, Inc.

Badr, H. M., Coutanceau, M., Dennis, S. C. R., & Mnard, C. (1990). Unsteady flow past a rotating circular

cylinder at Reynolds numbers 10 3 and 10 4. *Journal of Fluid Mechanics*, *220*, 459–484. https://doi.org/10.1017/S0022112090003342

Bergeson, L., & Kent Greenwald, C. (1985). Sail assist developments 1979-1985. *Journal of Wind Engineering and Industrial Aerodynamics*, *19*(1–3), 45–114. https://doi.org/10.1016/0167-6105(85)90056-X

Brasil Júnior, A. C. P. (2007). Modeling Of Hydrokinetic Turbine. In *COBEM 2007 - 19th International Congress of Mechanical Engineering*. Brasília, DF.

D'Alembert, J. le R. (1768). Paradoxe proposé aux géomètres sur la résistance des fluides. In *Opuscules mathématiques* (pp. 132–138). Paris: Briasson.

Goodwill, S. R., Chin, S. B., & Haake, S. J. (2004). Aerodynamics of spinning and non-spinning tennis balls. *Journal of Wind Engineering and Industrial Aerodynamics*, *92*(11), 935–958. https://doi.org/10.1016/j.jweia.2004.05.004

Huang, R. F., Cheng, J. C., Chen, J.-K., & Hsu, C. M. (2011). Manipulating flow to reduce drag of a square cylinder by using a self-sustained vibrating rod. *Journal of Fluids Engineering*, *133*(5), 051202-051202-14. https://doi.org/10.1115/1.4004091

Karabelas, S. J. (2010). Large Eddy Simulation of high-Reynolds number flow past a rotating cylinder. *International Journal of Heat and Fluid Flow*, *31*(4), 518–527. https://doi.org/10.1016/j.ijheatfluidflow.2010.02.010

Karabelas, S. J., Koumroglou, B. C., Argyropoulos, C. D., & Markatos, N. C. (2012). High Reynolds number turbulent flow past a rotating cylinder. *Applied Mathematical Modelling*, *36*(1), 379–398. https://doi.org/10.1016/j.apm.2011.07.032

Lugones, S. M. (2011). *Metodologia de Projeto Aerodinâmico de Pás de Turbinas Eólicas de Alto Desempenho*. Technological Inst. of Aeronautics (ITA), São José dos Campos, SP, Brazil.

Mannini, C., Marra, A. M., Pigolotti, L., & Bartoli, G. (2017). The effects of free-stream turbulence and angle of attack on the aerodynamics of a cylinder with rectangular 5:1 cross section. *Jnl. of Wind Engineering and Industrial Aerodynamics*, *161*, 42–58. https://doi.org/10.1016/j.jweia.2016.12.001

Munson, R. R., Young, D. F., & Okiishi, T. H. (2004). *Fundamentos da mecânica dos fluídos* (4th ed.). Edgard Blucher LTDA.

Murakami, N., & Ito, J. (2007). *US 20070046029 A1*.

Nagami, T., Higuchi, T., Nakata, H., Yanai, T., & Kanosue, K. (2016). Relation between lift force and ball spin for different baseball pitches. *Journal of Applied Biomechanics*, *32*(2), 196–204. https://doi.org/10.1123/jab.2015-0068

Prandtl, L. (1925). The Magnus effect and wind powered ships. *Naturwissenschaften*, *13*(6), 93–108. https://doi.org/10.1007/BF01585456

Reid, F. (1997). The Magnus Effect. *Parabola*, *33*(1).

Robertson, J. M., Wedding, J. B., Peterka, J. A., & Cermak, J. E. (1977). Wall pressures of separation - reattachment flow on a square prism in uniform flow. *Journal of Lndustrial Aerodynamics*, *2*(4), 345–359.

Tokumaru, P. T., & Dimotakis, P. E. (1991). Rotary oscillation control of a cylinder wake. *Journal of Fluid Mechanics*, *224*, 77–90. https://doi.org/10.1017/S0022112091001659

Vieira, R. C. C. (1961). *Contribuição ao estudo das aplicações dos cilindros rotativos.* Univ. of São Paulo, São Carlos, SP, Brazil.

Wobben, A. (2010). E-Ship 1 in testing phase. *Windblatt*, (02), 6–7.

Yen, S. C., San, K. C., & Chuang, T. H. (2008). Interactions of tandem square cylinders at low Reynolds numbers. *Experimental Thermal and Fluid Science*, *32*(4), 927–938. https://doi.org/10.1016/j.expthermflusci.2007.07.001

Zhang, P. F., Wang, J. J., Lu, S. F., & Mi, J. (2005). Aerodynamic characteristics of a square cylinder with a rod in a staggered arrangement. *Experiments in Fluids*, *38*(4), 494–502. https://doi.org/10.1007/s00348-005-0936-1